

# EXPERIMENTS AT GSI WITH ALADIN AND INDRA

W. Trautmann<sup>1</sup> for the ALADIN and INDRA-ALADIN collaborations

<sup>(1)</sup>Gesellschaft für Schwerionenforschung mbH, Planckstr. 1, D-64291 Darmstadt, Germany

The ALADIN and INDRA-ALADIN collaborations:

Dipartimento di Fisica dell' Università e I.N.F.N., I-95129 Catania, Italy

Forschungszentrum Rossendorf, D-01314 Dresden, Germany

Department of Physics and Astronomy and National Superconducting Cyclotron Laboratory,

Michigan State University, East Lansing, MI 48824, USA

Institut für Kernphysik, Universität Frankfurt, D-60486 Frankfurt, Germany

Istituto di Scienze Fisiche dell' Università e I.N.F.N., I-20133 Milano, Italy

Soltan Institute for Nuclear Studies, 00-681 Warsaw, Hoza 69, Poland

GANIL, CEA et IN2P3-CNRS, B.P. 5027, F-14076 Caen, France

LPC, IN2P3-CNRS, ISMRA et Université, F-14050 Caen, France

Niewodniczański Institute of Nuclear Physics, Pl-31342 Kraków, Poland

Dipartimento di Scienze Fisiche e INFN, Univ. Federico II, I-80126 Napoli, Italy

IPNO, IN2P3-CNRS et Université, F-91406 Orsay, France

DAPNIA/SPhN, CEA/Saclay, F-91191 Gif sur Yvette, France

IPNL, IN2P3-CNRS et Université, F-69622 Villeurbanne, France

## *Abstract*

The multi-fragment spectator decays following collisions of  $^{197}\text{Au}$  on  $^{197}\text{Au}$  and other heavy nuclei at relativistic bombarding energies have been studied by the ALADIN collaboration in recent years. The partitioning modes of the excited systems and their thermodynamic properties at breakup were in the center of interest in these experiments. Temperatures and excitation energies, but also breakup densities and emission times have been determined.

More recently, the multifragmentation of highly excited heavy nuclei was studied with the  $4\pi$  multidetector INDRA in experiments at the GSI in 1998 and 1999. The motivation for these new experiments was to extend the investigation of fragmentation processes and of their link to the liquid-gas phase transition to bombarding energies beyond those used in previous INDRA campaigns at GANIL. First results from the analysis of these data will be discussed with particular emphasis on topics related to previous ALADIN work.

## 1 INTRODUCTION

The experimental activity of the ALADIN collaboration has predominantly been focussed on the multi-fragment decays of excited spectator nuclei at relativistic bombarding energies [1-3]. Central  $^{197}\text{Au} + ^{197}\text{Au}$  collisions at lower bombarding energies and the phenomenon of collective radial flow [4, 5] as well as fission of  $^{238}\text{U}$  after Coulomb and nuclear excitations [6, 7] have also been studied.

The universality of the partitioning of the fragmenting systems, exhibited by the observed  $Z_{bound}$  scaling [1], was a prominent result of the initial experiments. This and other

indications of equilibrium have led to the investigation of the thermodynamic properties at breakup. Experimentally determined temperatures and excitation energies permitted the construction of a caloric curve of nuclei [8]. The measured densities, from correlation functions [9], and temperatures are consistent with a breakup within the coexistence zone of finite nuclei [10]. Valuable information on the mechanism of fragment formation is also provided by the kinetic energy spectra which seem to reflect the intrinsic Fermi motion within the system just before the onset of instabilities [11].

More recently, the multifragmentation of highly excited heavy nuclei was studied with

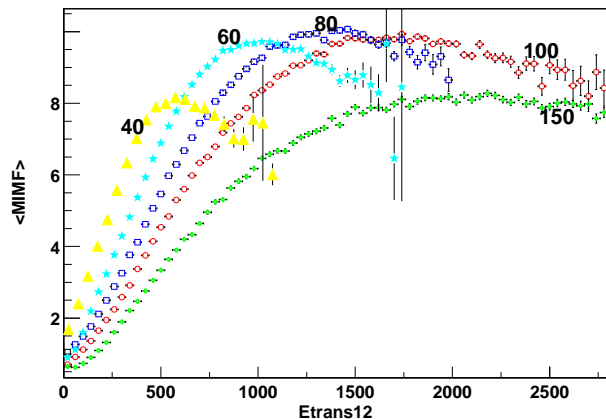


Figure 1: Mean multiplicity of intermediate-mass fragments ( $3 \leq Z \leq 30$ ) as a function of the transverse energy  $E_{\perp 12}$  of light particles ( $Z \leq 2$ ) for collisions of  $^{197}\text{Au} + ^{197}\text{Au}$  at  $E/A = 40, 60, 80, 100$  and  $150$  MeV.

the  $4\pi$  multidetector INDRA in experiments at the GSI between June 1998 and March 1999. The goal of these experiments was to extend the investigation of fragmentation processes, of the associated collective flow, of their link to the liquid-gas phase transition, and generally of the production and decay modes of heavy nuclei near their limit of stability to bombarding energies beyond those used in the previous INDRA experiments at GANIL.

As part of the INDRA@GSI campaign, fragmentation in asymmetric systems like  $^{12}\text{C} + ^{197}\text{Au}$  and  $^{12}\text{C} + ^{112,124}\text{Sn}$  was studied at bombarding energies ranging from 95 to 1800 MeV per nucleon. At angles  $\theta_{\text{lab}} \geq 45^\circ$ , the region of emissions from the target spectator, particle detection and identification with high resolution was achieved with the Si-Si-CsI(Tl) calibration telescopes of the INDRA multidetector system. These data offer a new perspective on spectator decays, provided by the detailed information from  $4\pi$  measurements in the laboratory frame.

For the future program of ALADIN, it is planned to include the projectile fragmentation of secondary beams available from the Fragment Separator FRS at GSI for the study of isotopic effects. For  $A = 124$  systems, e.g., a range of neutron-to-proton ratios  $N/Z$  from below 1.2 to 1.5 can be covered with secondary

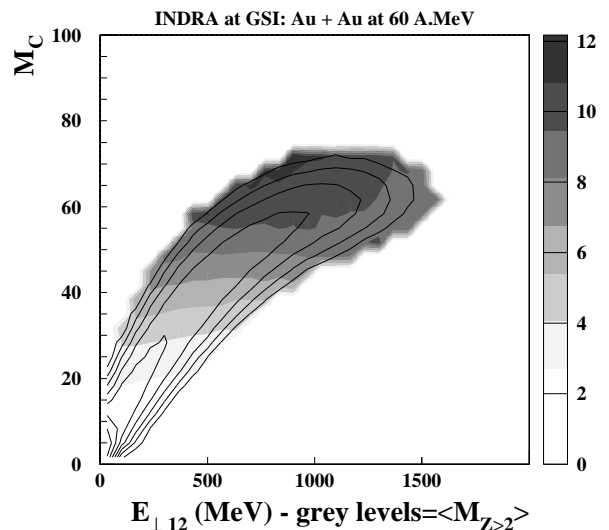


Figure 2: Double-differential reaction cross section (contour lines) and mean multiplicity of intermediate-mass fragments (shadings) as functions of the multiplicity of charged particles  $M_C$  and of the transverse energy  $E_{\perp 12}$  of light particles ( $Z \leq 2$ ) for  $^{197}\text{Au} + ^{197}\text{Au}$  collisions at  $E/A = 60$  MeV.

$^{124}\text{La}$  and stable  $^{124}\text{Sn}$  beams. Only rather low rates of incident projectile nuclei are required in inverse kinematics which facilitates such experiments with secondary beams.

The emphasis in this talk will lie on the new data obtained with INDRA, as far as possible, and on their relation to topics investigated in previous ALADIN experiments or in the planned isotopic studies. Some of the presented results are taken from ongoing analyses and, thus, should be considered as very preliminary. Results from the study of central and peripheral  $^{197}\text{Au} + ^{197}\text{Au}$  collisions in the range of bombarding energies  $40 \text{ MeV} \leq E/A \leq 150$  MeV are presented by J. Łukasik in his contribution to this workshop [12].

## 2 THE RISE AND FALL IN CENTRAL COLLISIONS

The rise and fall of the observed fragment multiplicity with increasing violence of the collision has been observed in the first experiments with ALADIN [15]. It reflects the evolution of the dominant decay modes from con-

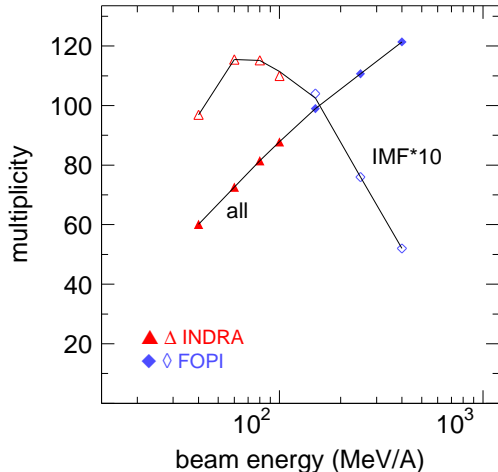


Figure 3: Mean multiplicities of charged particles (full symbols) and intermediate-mass fragments (open symbols, scaled up by a factor of 10) for central  $^{197}\text{Au} + ^{197}\text{Au}$  collisions as a function of the bombarding energy. The data for  $E/A \geq 150$  MeV have been measured by the FOPI collaboration [13].

ventional evaporation through multifragmentation ('cracking') towards the nearly complete disintegration into light particles and clusters ('vaporization') that has been predicted by statistical multifragmentation models [16, 17].

With the MSU/WU Miniball/wall coupled to the ALADIN forward spectrometer, the characteristics of the fragmentation channels were studied as a function of the bombarding energy and the impact parameter [18]. At the lowest energy  $E/A = 100$  MeV covered in these experiments, the highest fragment multiplicities were observed in central collisions, associated with a considerable collective component in the fragment motion and with exponential charge spectra which both distinguish these decay modes from those following spectator excitations [4, 5].

The new INDRA data cover the range  $40 \text{ MeV} \leq E/A \leq 150$  MeV and thus extend to even lower energies. The measured fragment multiplicities ( $3 \leq Z \leq 30$ ) are shown in Fig. 1 as a function of the transverse energy  $E_{\perp 12}$  of light charged particles ( $Z \leq 2$ ) which was chosen here as an impact parameter selector. They are not corrected for the acceptance of the INDRA detector, but it turns out that

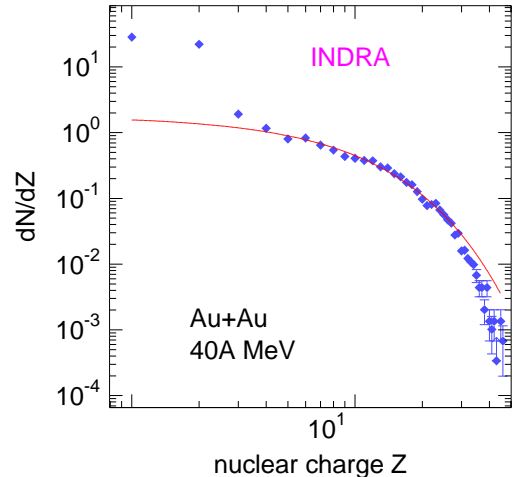


Figure 4: Spectrum of fragment atomic numbers  $Z$  for central collisions of  $^{197}\text{Au} + ^{197}\text{Au}$  at  $E/A = 40$  MeV. The exponential curve has been adapted to the region of intermediate-mass fragments.

nearly 90% of the total charge of the collision system is collected in the most violent collisions. The maximum multiplicity is reached for bombarding energies of 60 to 80 MeV per nucleon but not for collisions with the largest transverse energy. An anticorrelation seems to exist between the number of fragments and the transverse energy observed in the light-particle channels which is strongest at the lowest bombarding energies. There, apparently, the fragment production is governed by the amount of dissipated energy that is left available.

A different representation of the same feature is given in Fig. 2. The ridge line of the cross section distribution as a function of the multiplicity of charged particles  $M_C$  and of the transverse energy  $E_{\perp 12}$  of light particles ( $Z \leq 2$ ) saturates in  $M_C$  for central collisions. The highest multiplicities of intermediate-mass fragments are observed for largest  $M_C$  but, for given  $M_C$ , for the smallest  $E_{\perp 12}$ .

Selecting only central collisions, the mean fragment multiplicities describe a rise and fall as a function of the incident energy but drop rather rapidly once the relativistic regime is reached. This is illustrated in Fig. 3 in which the new data of the INDRA@GSI campaign are combined with the FOPI data measured

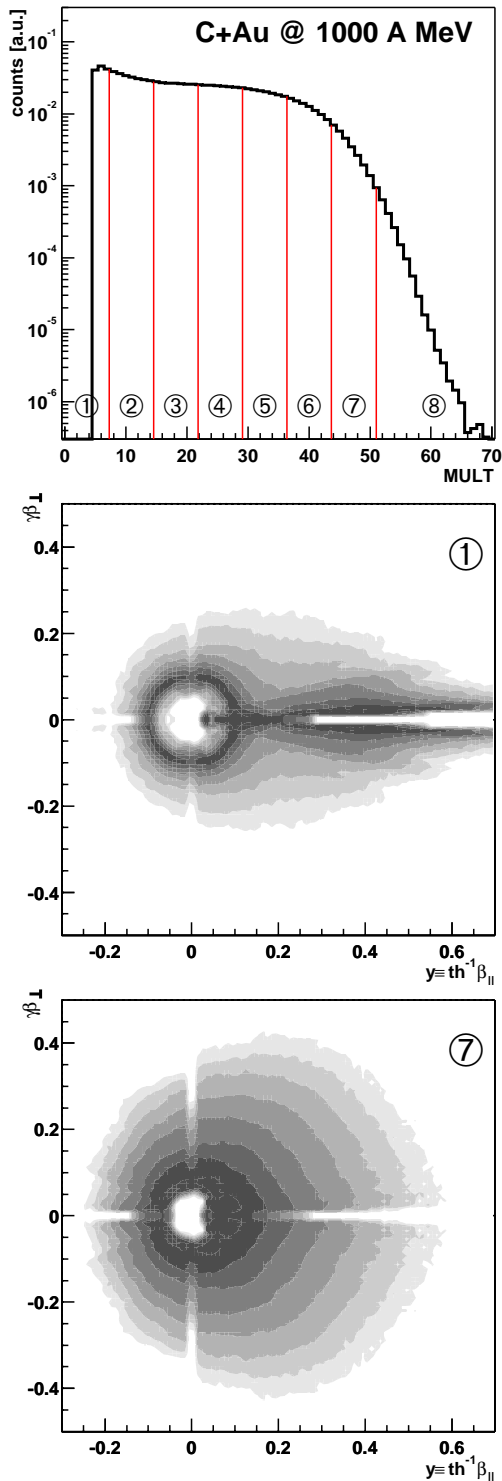


Figure 5: Illustration of the impact parameter selection using the multiplicity of charged particles ( $Z \geq 1$ , top panel) and examples of invariant distributions of helium clusters for peripheral (bin 1, middle panel) and central (bin 7, bottom panel) collisions of  $^{12}\text{C} + ^{197}\text{Au}$  at  $E/A = 1000$  MeV. The grey shadings follow a logarithmic scale.

for  $150 \leq E/A \leq 400$  MeV [13]. The fragment charge distributions at the higher energies are exponential with rapidly increasing steepness, a trend continued to AGS energies [14]. As illustrated in Fig. 4, nearly exponential spectra shapes, often associated with the existence of collective flow [5, 19], are also observed at the lower bombarding energy where flow is nearly nonexistent [12]. They are well described by the statistical fragmentation model, however, without explicitly including the coupling between the partitioning and the collective motion. The question of the shapes of these spectra thus remains intriguing in itself.

### 3 EQUILIBRIUM IN SPECTATOR DECAYS

Indications of equilibrium in spectator decays have been derived from the universality of the partitioning and from the invariance of the fragment kinetic energies with the incident energy [1]. It does not extend to the light particles emitted at spectator rapidities. The separation of equilibrium and preequilibrium emissions, however, is crucial for thermodynamic analyses at the breakup state (see next section).

The high values of the inverse slope parameters of proton spectra [11] as well as the bombarding energy dependence of the neutron emissions [20], both observed at spectator rapidities, were clear indications of the contributions from the initial reaction stages to this kinematic regime. The question of equilibrium in light-charged-particle emissions can be studied more precisely in the laboratory frame. This is illustrated in Fig. 5 where invariant-velocity distributions of helium particles for peripheral and central collisions of  $^{12}\text{C} + ^{197}\text{Au}$  at 1000 MeV per nucleon are shown. The spectra of, mostly,  $\alpha$  particles from the breakup of the projectile and its interactions with the target in peripheral collisions at very forward angles extend over a large range of energies ( $y_{\text{proj}} = 1.36$ ). In central collisions, a preequilibrium component, spread out over

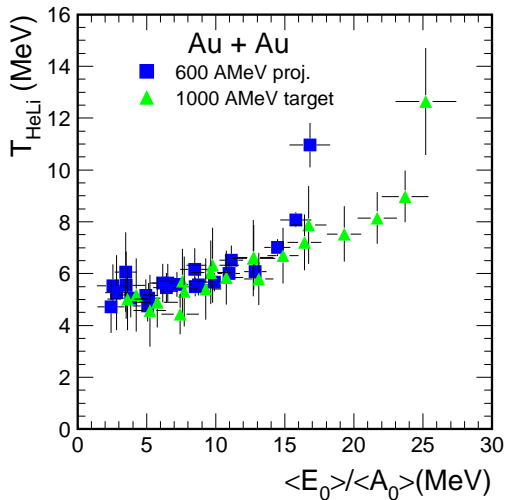


Figure 6: Caloric curve of nuclei as given by the temperature  $T_{\text{HeLi}}$  as a function of the measured excitation energy per nucleon for  $^{197}\text{Au} + ^{197}\text{Au}$  collisions at  $E/A = 600$  MeV and 1000 MeV. (from Ref. [25]).

the forward hemisphere, is superimposed over the isotropic equilibrium emissions at target rapidities. These components are not easily separated with moving-source fits because the preequilibrium component is not isotropic.

#### 4 THE NUCLEAR CALORIC CURVE

The caloric curve of nuclei, obtained for  $^{197}\text{Au} + ^{197}\text{Au}$  collisions at 600 MeV per nucleon, has demonstrated that temperature-sensitive observables exist that can be used over practically the full range of decay modes from compound emissions to nearly complete vaporization [8]. It has been noted later on that the calorimetric determination of the excitation energy, even if it is restricted to the spectator kinematic regime, will lead to results that do not reflect the universality of the partition patterns (Fig. 6).

The application of corrections for preequilibrium emissions requires an adequate understanding of the reaction stages prior to breakup (cf. preceding section) and of the origin of the particle and fragment kinetic energies (next

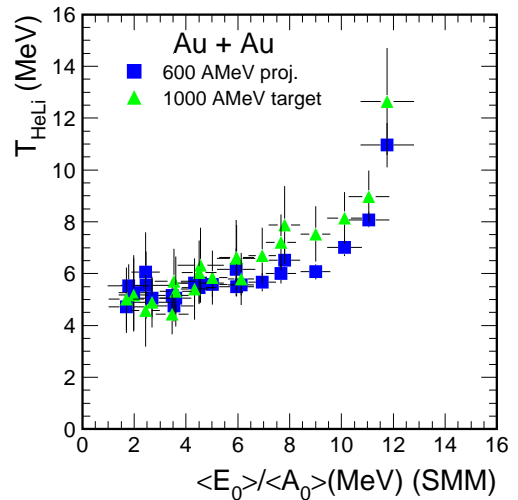


Figure 7: Caloric curve of nuclei for  $^{197}\text{Au} + ^{197}\text{Au}$  collisions at  $E/A = 600$  MeV and 1000 MeV as obtained by using the excitation energy per nucleon from the SMM reconstruction. (from Ref. [25]).

section). In this situation, it is useful to refer to model predictions for the excitation energies required for the observed breakup channels. It has been shown that the statistical fragmentation model can reproduce the measured charge correlations including their dispersions around the mean values to high accuracy [21]. With the model parameters adjusted in this way, the evolution of the breakup temperature with excitation energy and its relation to the experimental isotope temperature  $T_{\text{HeLi}}$  have been studied [22, 23]. The caloric curve obtained in this way is invariant with the bombarding energy, a consequence of the universality of the fragmentation pattern (Fig. 7). Further results for several different reactions are presented by G. Imme at this workshop [24].

#### 5 KINETIC ENERGIES IN SPECTATOR DECAYS

The kinetic energies of the fragments and light charged particles from the decay of target spectators in  $^{197}\text{Au} + ^{197}\text{Au}$  collisions at 1000 MeV per nucleon have been measured in a previous ALADIN experiment with high-

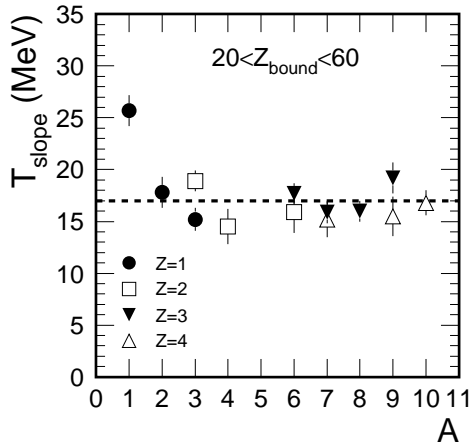


Figure 8: Slope temperatures for isotopically resolved charged particles and fragments, measured at  $\Theta_{lab} = 150^\circ$ , as a function of the mass number  $A$  for  $^{197}\text{Au} + ^{197}\text{Au}$  collisions at  $E/A = 1000$  MeV. For protons and  $\alpha$  particles the value of the high-temperature component is shown (from Ref. [11]).

resolution telescopes at backward angles [11]. Except for protons and apart from the observed evaporation components, the kinetic-energy spectra were found to exhibit slope temperatures of about 17 MeV and invariant with the particle species (Fig. 8). It was suggested that these slope temperatures may reflect the intrinsic Fermi motion of the spectator system at the instant of its becoming unstable. An interpretation within the Goldhaber model [26], extended to the case of expanded fermionic systems at finite temperature [27], was able to account for the slope temperatures and the isotope temperature  $T_{\text{HeLi}}$ , and for their correlated dependence on the impact parameter. An explanation along similar lines has been presented by Gaitanos et al. [28].

The new measurements with INDRA for target spectators in the  $^{12}\text{C} + ^{197}\text{Au}$  reactions confirm these interpretations. At incident energies equal or exceeding 300 MeV per nucleon, the measured slope temperatures were found to be also virtually invariant with the bombarding energy. The values for, e.g.  $^7\text{Li}$  near  $\theta_{lab} = 100^\circ$ , are 14.0, 18.5 and 18.4 MeV at 300, 600, and 1000 MeV per nucleon, respectively [29]. The incident energy, apparently, is not strongly influencing the fragment kinetic en-

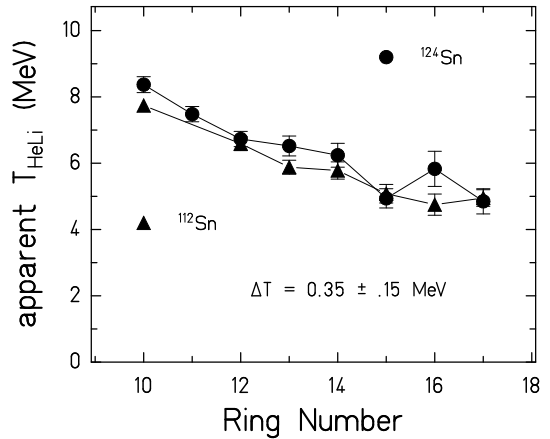


Figure 9: Apparent isotopic temperature  $T_{\text{HeLi}}$  as a function of the INDRA ring number for the reactions  $^{12}\text{C} + ^{112,124}\text{Sn}$  at  $E/A = 300$  MeV.

ergies. At more forward angles, the contributions from preequilibrium emissions at peripheral impact parameters lead to energy spectra that are nearly flat up to the detection limits of the INDRA detectors.

## 6 OUTLOOK: ISOTOPIC EFFECTS AND EXPERIMENT S254

Isotopic effects in nuclear reactions are receiving increasing attention because of their relation with the symmetry energy in the nuclear equation of state whose density dependence is of high current interest, in particular also for astrophysical applications [30]. The ALADIN collaboration has proposed a comparative study of the multifragmentation of spectator systems at relativistic energies with primary stable beams of  $^{124}\text{Sn}$  and with secondary beams of  $^{124}\text{La}$  produced in the fragmentation of primary  $^{142}\text{Nd}$ . In addition, the dependence of the thermodynamic observables on the mass of the primary fragmenting system will be investigated with  $^{124}\text{Sn}$  and  $^{197}\text{Au}$  projectiles which have very similar  $N/Z \approx 1.5$ .

Preliminary answers to some of these questions may be obtained from the INDRA@GSI data collected for  $^{12}\text{C} + ^{112,124}\text{Sn}$  reactions at 300 and 600 MeV per nucleon. The difference in isospin of the two tin targets is smaller

than that of the projectiles for the new experiment. However, a variety of interesting isotopic effects has already been observed in experiments with the two tin and other stable, isotopically pure, targets and beams (see, e.g., Ref. [31, 32]). The phenomenon of isoscaling in light-ion induced reactions on  $^{112,124}\text{Sn}$  targets and its statistical interpretation are discussed by A. Botvina [33].

Preliminary results for the apparent isotope temperature  $T_{\text{HeLi}}$  for  $^{12}\text{C} + \text{Sn}$  at 300 MeV per nucleon are shown in Fig. 9. For each of the rings 10 to 17 of INDRA ( $\theta_{\text{lab}} \geq 45^\circ$ ), the isotopically resolved spectra of helium and lithium isotopes measured with the calibration telescopes were extrapolated with Maxwell-Boltzmann fits, and their integrated yields were determined. Whereas the individual helium and lithium yield ratios depend more strongly on the isotopic composition of the target only a small effect is seen in the double ratio from which the temperature is derived. The predictions for this temperature difference depend on what is assumed to be the determining factor, the temperature limiting the existence of a self-bound object according to finite-temperature Hartree-Fock calculations [34] or the number of degrees of freedom of the fragmented system over which the available energy is distributed. The limiting temperatures calculated by Besprosvany and Levit [35] differ by about 1 MeV for these nuclei while the statistical multifragmentation model predicts much smaller differences.

*The authors would like to thank W. Reisdorf for useful discussions and for providing us with graphics for this talk.*

## REFERENCES

- [1] A. Schüttauf et al., Nucl. Phys. A 607(1996)457.
- [2] J. Pochodzalla, Prog. Part. Nucl. Phys. 39(1997)443.
- [3] W. Trautmann, in Correlations and Clustering Phenomena in Subatomic Physics, edited by M.N. Harakeh et al. (Plenum Press, 1997), p. 115.
- [4] W.C. Hsi et al., Phys. Rev. Lett. 73(1994)3367.
- [5] G.J. Kunde et al., Phys. Rev. Lett. 74(1995)38.
- [6] Th. Rubehn et al., Z. Phys. A 353(1995)197.
- [7] Th. Rubehn et al., Phys. Rev. C 53(1996)3143.
- [8] J. Pochodzalla et al., Phys. Rev. Lett. 75(1995)1040.
- [9] S. Fritz et al., Phys. Lett. B 461(1999)315.
- [10] W. Trautmann, Nucl. Phys. A 685(2001)233c.
- [11] T. Odeh et al., Phys. Rev. Lett. 84(2000)4557.
- [12] J. Lukasik et al., contribution to this workshop.
- [13] W. Reisdorf et al., Nucl. Phys. A 612(1997)493.
- [14] T.A. Armstrong et al., Phys. Rev. Lett. 83(1999)5431.
- [15] C. Ogilvie et al., Phys. Rev. Lett. 67(1991)1214.
- [16] D.H.E. Gross et al., Phys. Rev. Lett. 56(1986)1544.
- [17] J.P. Bondorf et al., Phys. Rep. 257(1995)133.
- [18] M.B. Tsang et al., Phys. Rev. Lett. 71(1993)1502.
- [19] S. Chikazumi et al., Phys. Lett. B 476(2000)273.
- [20] W. Trautmann et al., in Proceedings of the XXXV International Winter Meeting on Nuclear Physics, Bormio, 1997, edited by I. Iori (Ricerca Scientifica ed Educazione Permanente, 1997), p. 441.
- [21] A.S. Botvina et al., Nucl. Phys. A 584(1995)737.
- [22] Hongfei Xi et al., Z. Phys. A 359(1997)397.
- [23] Al.H. Raduta and Ad.R. Raduta, Phys. Rev. C 61(2000)034611.
- [24] G. Immé et al., contribution to this workshop.
- [25] T. Odeh, Ph.D. thesis, Universität Frankfurt, 1999.
- [26] A.S. Goldhaber, Phys. Lett. 53B(1974)306.
- [27] W. Bauer, Phys. Rev. C 51(1995)803.
- [28] T. Gaitanos et al., Phys. Lett. B 478(2000)79.
- [29] K. Turzó et al., in Proceedings of the XXXIX International Winter Meeting on Nuclear Physics, Bormio, 2001, edited by I. Iori and A. Moroni (Ricerca Scientifica ed Educazione Permanente, 2001), p. 152.
- [30] H. Müller and B.D. Serot, Phys. Rev. C 52(1995)2072.
- [31] M.B. Tsang et al., Phys. Rev. Lett. 86(2001)5023.
- [32] F. Rami et al., Phys. Rev. Lett. 84(2000)1120.
- [33] A.S. Botvina et al., contribution to this workshop and nucl-th/0112049.
- [34] J.B. Natowitz et al., Phys. Rev. C 52(1995)R2322.
- [35] J. Besprosvany and S. Levit, Phys. Lett. B 217(1989)1.